ORGANIC CHEMISTRY
FRONTIERS

RESEARCH ARTICLE

View Article Online
View Journal | View Issue

Cite this: *Org. Chem. Front.*, 2022, **9**, 1327

A cucurbit[8]uril-stabilized 3D charge transfer supramolecular polymer with a remarkable confinement effect for enhanced photocatalytic proton reduction and thioether oxidation†

Zhuo Lei, Qian Li, Jian-Da Sun, Ze-Kun Wang, Hui Wang, Zhan-Ting Li * and Dan-Wei Zhang *

Received 29th December 2021,
Accepted 19th January 2022

DOI: 10.1039/d1qo01939b

rsc.li/frontiers-organic

A highly water-soluble tetrahedral compound T1 that contains one tetraphenylmethane core and four 2-oxynaphthelene-CH_2-4,4′-bipyridinium (NP-CH_2-DIPY) side arms has been prepared. Control experiments reveal that NP-CH_2-BIPY undergoes antiparallel dimerization which is stabilized by two charge transfer interactions with NP as an electron-rich donor and BIPY as an electron-deficient acceptor. This binding motif drives T1 to aggregate into a nanoscale supramolecular polymer SP in water. Adding 2 equivalents of cucurbit[8]uril to the solution of SP leads to the formation of a more stable three dimensional supramolecular polymer CBSP through a 2 + 2 binding motif in which two CB[8] rings encapsulate one charge transfer complex formed by the antiparallel NP-CH_2-DIPY dimer. As a water soluble porous supramolecular polymer, CBSP exhibits a remarkable confinement effect for visible light-induced proton reduction to produce hydrogen and ʟ-methionine thioether oxidation to the corresponding sulfoxide derivative in water.

Introduction

Supramolecular polymers have emerged from the combination of conventional covalently bonded polymers and non-covalent bonding motifs.[1–11] Pioneering works by Lehn and Meijer triggered extensive investigations of hydrogen bonding as a driving force for the generation of supramolecular polymers,[12–15] which were followed by the applications of other non-covalent forces, including coordination,[16,17] donor–acceptor interaction,[18,19] solvophobicity[20–22] and ionic pairing electrostatic interaction.[23–26] Most of the early reports of supramolecular polymers have been realized in organic media of low polarity. Hydrophobicity provides the most efficient approach to construct supramolecular polymers in water.[27–29] In this context, many robust connecting patterns have been developed through encapsulation of cyclodextrins and cucurbiturils for hydrophobic monomeric or dimeric species.[21,30–36] The application of polymeric and multitopic building blocks has allowed for the fabrication of three-dimensional (3D) supramolecular polymers in water with enhanced stability that is not attainable for linear systems. In recent years, such 3D supramolecular polymers have been vigorously investigated as biocompatible materials for self-healing, drug delivery and bioimaging.[37–40] Further development of 3D water-soluble, porous supramolecular polymers should open new opportunities for the exploration of novel porosity-based functions in aqueous media. Currently, examples of the application of supramolecular polymers for homogeneous catalysis in aqueous media are very rare.[41,42] To expand this potential, the establishment of new binding patterns for the construction of functional supramolecular architectures is highly desirable.

We previously reported the generation of water-soluble, three-dimensional supramolecular polymers from the co-assembly of cucurbit[8]uril (CB[8]) and rationally designed multitopic building blocks,[43–45] which is driven by the encapsulation of the CB[8] macrocycle for intermolecular homodimers of peripheral hydrophobic aromatic units of the multitopic building blocks.[30–32] Given the high stability of the 2 + 2 complexation patterns formed between CB[8] and elongated aromatic guests,[46–51] we envisioned that the implementation of this enhanced binding motif might lead to the generation of new, highly stable 3D supramolecular polymers that exhibit unique functions. We herein describe that a tetraphenylmethane-cored compound that bears four donor–acceptor-type side arms can co-assemble with CB[8] in water to form a

---

Department of Chemistry, Shanghai Key Laboratory of Molecular Catalysis, Fudan University, Shanghai 200438, China. E-mail: zhangdw@fudan.edu.cn, ztli@fudan.edu.cn

† Electronic supplementary information (ESI) available: Synthesis and characterization of new compounds and ^1H and ^{13}C NMR and dynamic light scattering profiles. See DOI: 10.1039/d1qo01939b

highly stable charge transfer complexation-based porous supramolecular polymer, which exhibits a remarkable confinement effect in water for enhanced visible light-induced proton reduction and thioether oxidation to afford hydrogen gas and a sulfone.

Results and discussion

When an electron-rich aromatic unit is connected to an electron-deficient aromatic unit with a short linker that does not allow for intramolecular interaction, the resulting ditopic molecule may stack to form a homodimer stabilized by two intermolecular donor–acceptor interactions or charge transfer complexations.[46–51] The encapsulation of one CB[8] macrocycle for the single donor–acceptor complex can further stabilize the whole dimer through multivalency.[52,53] Zhang *et al.* utilized this strategy to construct a main-chain supramolecular polymer from 1′,1″-(butane-1,4-diyl)bis(1-(anthracen-2-ylmethyl)-4,4′-bipyridine-1,1′-diium) bromide.[54] To develop a new binding motif to fabricate highly stable 3D supramolecular polymers in water, we designed and synthesized a tetrahedral compound **T1** which bears four hydrophilic diglycol chains (Scheme 1). It was envisioned that the 2-oxynaphthelene and 4,4′-dipyridinium units in the four peripheral aromatic arms would undergo intermolecular dimerization which could be further stabilized by two CB[8] macrocycles to afford a 3D donor–acceptor-type supramolecular polymer.

The synthetic route to compound **T1** is shown in Scheme 1. Compounds **1** and **2**[55] were condensed in acetonitrile under reflux to afford compound **3** in 83% yield. Compound **3** was then reduced with $LiAlH_4$ in tetrahydrofuran to give compound **4** in 97% yield. The treatment of **4** with phosphorus tribromide produced **5** in 58% yield. Finally, compound **5** was condensed with **6**[56] in *N*,*N*-dimethylformamide to afford **T1** in 66% yield, which had good solubility in water (>2.5 mM). Compounds **M1**, **M2** and **BVM** were prepared as control molecules. The details for their synthesis are provided in the ESI.†

The ^1H NMR spectrum of compound **T1** in D_2O exhibited one set of signals. When CB[8] was added to the solution, the resolution of the signals continuously decreased and the spectrum of their 1 : 4 mixture only gave rise to broad unidentifiable signals (Fig. S1†). This observation indicated that strong binding occurred between the two compounds, but the binding stoichiometry could not be established. Thus, ^1H NMR titration experiments were carried out for control **M1** and CB[8] in D_2O. Upon the addition of CB[8], a new set of signals appeared, whereas those of free **M1** became weakened (Fig. 1a). With the increase of the amount of CB[8], this set of signals became enhanced, but did not undergo any shifting. When 1.0 equivalent of CB[8] was added, the signals of free **M1** vanished completely. Adding another 1.0 equivalent of CB[8] did not cause the generation of new signals. These results confirmed that the two components formed a very stable 2 + 2 complex, which did not undergo quick exchange with the free components on the ^1H NMR timescale. The

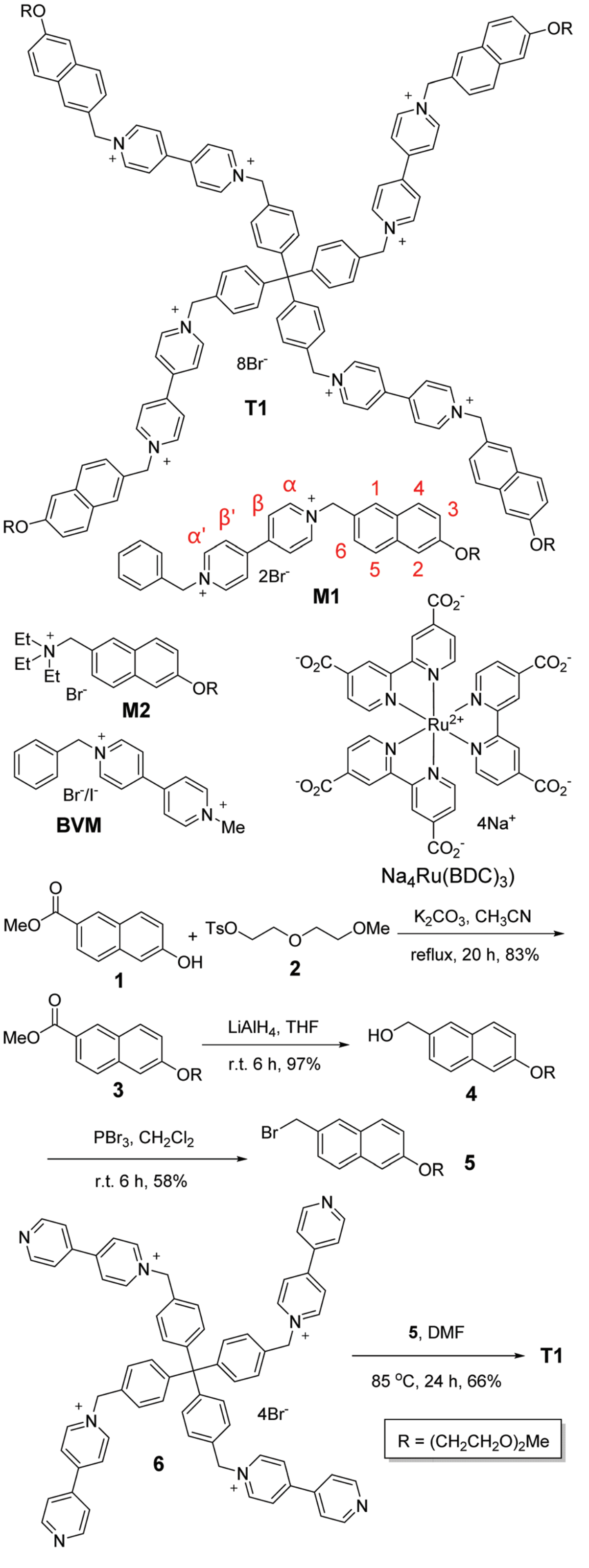

Scheme 1 The structures of compounds **T1**, **M1**, **M2**, **BVM** and $Na_4[Ru(BDC)_3]$ and the synthetic route to compound **T1**.

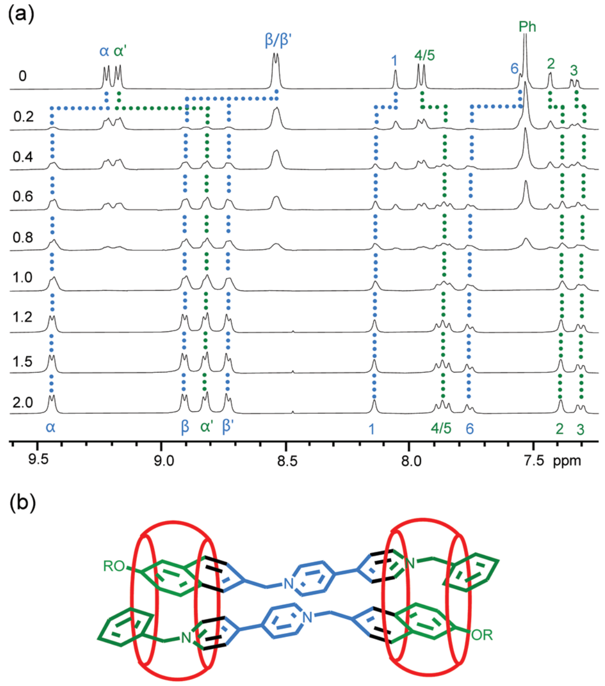

Fig. 1 (a) ^{1}H NMR spectra of the mixture of **M1** (5.0 mM) and CB[8] (0, 0.2, 0.4, 0.6, 0.8, 1.0, 1.2, 1.5 and 2.0 equiv.) in D_2O at 25 °C. (b) 2 + 2 binding pattern between **M1** and CB[8] revealed by the above ^{1}H NMR spectra in D_2O, highlighting a slipped antiparallel stacking of the aromatic units of two molecules of **M1** in the cavity of the CB[8] macrocycles.

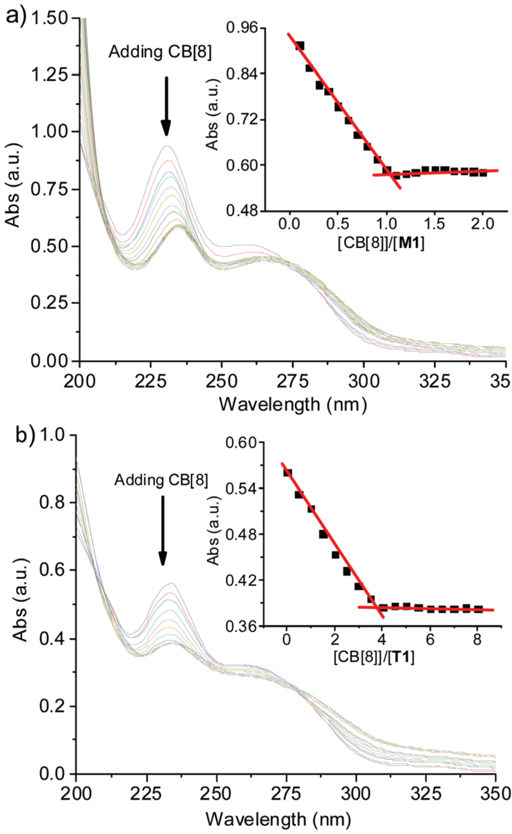

Fig. 2 UV–vis absorption spectra of (a) **M1** (20 μM) and (b) **T1** (2.5 μM) in water in the presence of an incremental amount of CB[8] at 25 °C. Inset: the absorbance at 233 nm *vs.* [CB[8]]/[**M1**] or [**T1**].

signals of **M1** within the downfield area in the CB[8]-free solution and the solution of its 1 : 1 mixture were assigned using the 2D NMR technique (Fig. S2 and S3†). A comparison of the two spectra revealed that the signals of α′- and 2–5-H of **M1** underwent significant upshifting, which can be attributed to the shielding of the CB[8] macrocycle through encapsulation. In contrast, the signals of α-, β-, β′-, 1- and 6-H shifted downfield pronouncedly, which could be caused by the de-shielding of the CB[8] macrocycle and possibly also by forming intermolecular hydrogen bonding with the carbonyl oxygen atoms of CB[8]. These results supported that the two compounds formed a 2 + 2 complex with the binding pattern shown in Fig. 1b.

UV-vis spectra were then recorded for both **M1** and **T1** with the addition of an incremental amount of CB[8] (Fig. 2). For both compounds, adding CB[8] caused a significant decrease of the absorption centred at 233 nm, which gave an inflection point when 1.0 or 4.0 equiv. of CB[8] were added. This is because **T1** bears four side arms that can bind to CB[8]. These results indicated that both compounds formed stable complexes with CB[8] at the respective low concentration. By assuming a low limit of 95% of the two components that formed the 2 + 2 complexes, the association constant (K_a) for the four-component complex $(\mathbf{M2})_2{\subset}(\mathrm{CB[8]})_2$ could be calculated to be 1.9×10^{16} M^{-3}, whereas the apparent K_a for the similar complexes formed by the side arms of **T1** and CB[8] was determined to be 1.5×10^{17} M^{-3}. The latter was substantially larger than the former, well reflecting the multivalency of the tetratopic molecule in binding to CB[8].

2,6-Dialkoxynaphthalene has been demonstrated as an electron-rich aromatic unit to produce intermolecular donor–acceptor complexes.[46,57–59] We conjectured that the 2-alkoxynaphthalene unit at a high concentration might also function as an electron-rich donor to form similar complexes, which can be further enhanced through CB[8] encapsulation in water. We thus further recorded the UV-vis absorption spectra of **M1** and **T1** at high concentrations. The UV-vis absorption spectrum displayed a broad absorption band around 390 and 408 nm (Fig. 3a), respectively. Adding 1.0 or 4.0 equivalents of CB[8] to their solution caused significant enhancement of this absorption band and the maximum absorption wavelength also shifted to 405 and 420 nm, respectively. With or without the addition of CB[8], this absorption band exhibited an identical molar absorption coefficient (ε) that was independent of the concentration (Fig. S4–S7†). For **T1**, the ε values were 393 and 206, and for **M1**, the values were 134 and 62. Consistent with the above observations, the aqueous solutions of compounds **T1** and **M1** were brown and light brown (Fig. 3b), which were dependent on the concentration, while adding CB[8] caused darkening of the colour. Because both controls

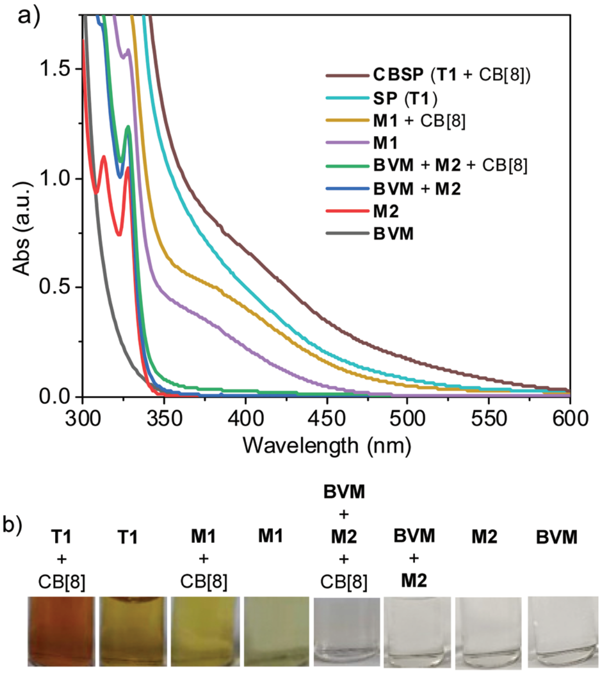

Fig. 3 (a) UV/vis absorption spectrum of the solution of **CBSP** (**T1** + 2CB[8]), **SP** (**T1**), **M1** + CB[8], **M1**, **BVM** + **M2** + CB[8], **BVM** + **M2**, **M2** and **BVM** in water. For all the solutions, the concentration of the NP and/or BIPY units was kept at 1.0 mM. (b) The photographs of the different solutions highlighting their colours. For all the solutions, the concentration of the BIPY unit was controlled at 5.0 mM.

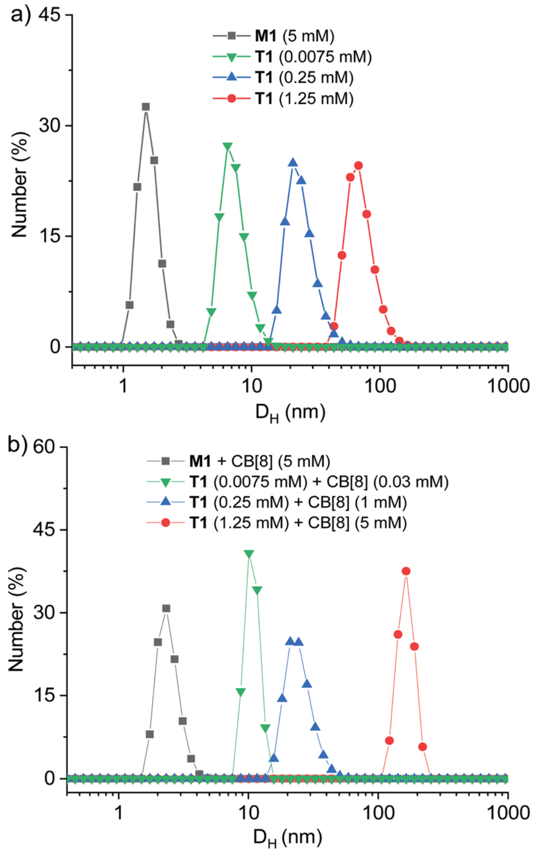

Fig. 4 Dynamic light scattering profile of (a) the solution of **M1** and **T1** in water and (b) the solution of the mixture of **M1** (1 : 1) and **T1** (1 : 4) with CB[8] in H_2O at 25 °C.

M2 and **BVM** did not exhibit significant absorption within the range of long wavelengths (>350 nm) (Fig. 3a and b), these results supported that both **M1** and **T1** formed charge transfer complexes, which were further strengthened by CB[8]. These observations showed that encapsulation complexation of CB[8] for the donor–acceptor dimer of **M1** was remarkably enhanced in the 2 + 2 binding as compared with the simple three-component complexation. The results also showed that the charge transfer complexes formed by **T1** was more stable than those of **M1** in the absence or presence of CB[8].

Since the UV-vis absorption spectra could not be recorded for the solution of even higher concentrations, we then conducted ^{1}H NMR experiments for the solution of **M1** and **T1** at concentrations higher than those used for the above UV-vis spectroscopy. When the concentration of **T1** was increased from 0.5 mM to 2.5 mM, which corresponded to the concentration of 2.0 and 10 mM for the appended aromatic arms, the signals of the protons of the bipyridinium and naphthalene units in the ^{1}H NMR spectrum all underwent significant upshifting (0.1–0.6 ppm) (Fig. S8†). Accompanied by this continuous upshifting of the signals, their resolution also decreased gradually, indicating increasing intermolecular stacking. In contrast, for **M1**, increasing the concentration from 2 mM to 10 mM did not cause large shifting of the signals of the two aromatic units (Fig. S9†). These results further confirmed that the bipyridinium and naphthalene units of **T1** formed more stable charge transfer complexes.

Dynamic light scattering (DLS) experiments further revealed the formation of large aggregates by **T1** in the absence and presence of CB[8] (Fig. 4). At a high concentration of 5.0 mM, the solution of **M1** gave rise to a very small hydrodynamic diameter (D_H) of 1.5 nm. With the addition of 1.0 equivalent of CB[8], D_H was increased slightly to 2.3 nm, which was still very small. In contrast, at a concentration of 1.25 mM, which corresponded to the concentration of 5 mM for the four side arms, the D_H value was determined to be 68 nm. With the addition of CB[8] (5 mM), the D_H value was increased to 165 nm. Both results reflected that **T1** itself underwent significant aggregation to afford nanoscale supramolecular entities, which were converted into even large supramolecular entities through binding with CB[8]. As expected, diluting the solution caused the decrease of the D_H value for both **T1** and its mixture with CB[8] (Fig. 4 and S10†). However, even at a low concentration of 0.0075 mM, two solutions still gave rise to D_H of 6.5 and 10 nm. Taken together, the above ^{1}H NMR, UV-vis and DLS experiments consistently supported that **T1** aggregated in water to afford a charge transfer-type supramolecular polymer **SP** and its 1 : 4 mixture with CB[8] gave rise to a more stable and even larger 3D supramolecular polymer **CBSP** (Fig. 5). Given the tendency of tetrahedral building blocks to form 3D porous architectures in solutions, we propose that the 3D

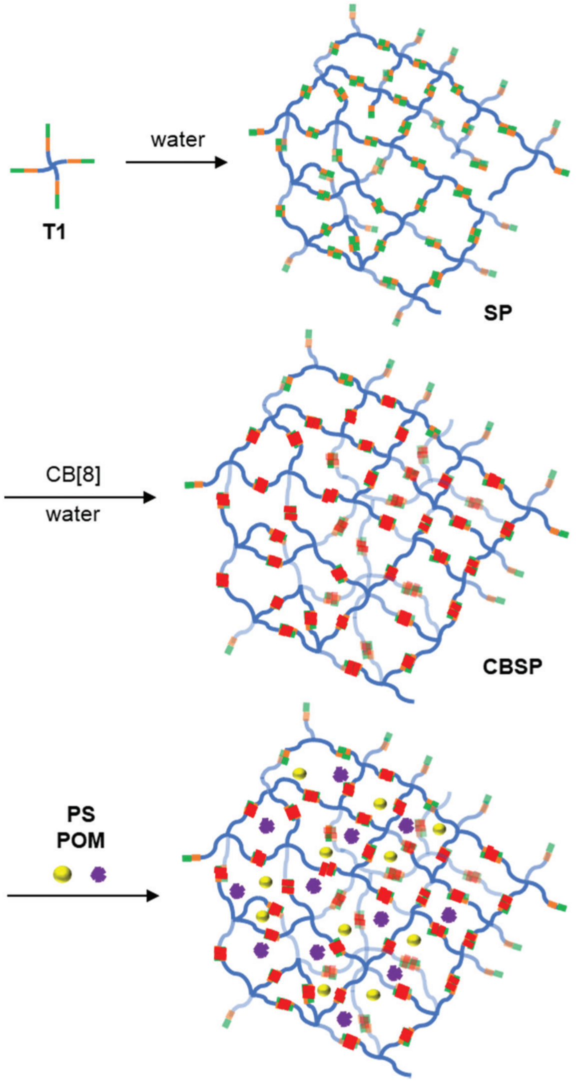

Fig. 5 Representation of the self-assembly of the 3D supramolecular polymer **CBSP** from **T1** and CB[8] in water and its inclusion of the photosensitizer and the **POM** catalyst.

supramolecular polymers formed by **T1** and CB[8] should possess intrinsic porosity. By assuming an ideal 3D diamondoid structure, **CBSP** would form porous channels with an aperture diameter of 4.0 nm (Fig. S11†).

Porous organic polymers are ideal materials for the attainment of the confinement effect for catalysing various heterogeneous chemical transformations.[60–65] We have also demonstrated that homogeneous 3D porous supramolecular organic frameworks can exhibit an important confinement effect for homogeneous photocatalysis in aqueous media.[66–69] The high stability of **CBSP** allows it to maintain a nanoscale size at micromolar concentrations of the building blocks. We thus studied the capability of **CBSP** for simultaneous enrichment of the photosensitizer $Na_4[Ru(BDC)_3]$ (**PS**, BDC = 2,2′-bipyridyl-4,4′-carboxylate) (Scheme 1) and the Keggin-type polyoxometalate catalyst $Na_3PW_{12}O_{40}$ (**POM**), which forms an important integrated photocatalytic system for visible light induced reduction of protons into H_2.[67,70] This enrichment was expected to take place due to the multianionic character of both species, which should lead to the inclusion of the two species in the interior of **CBSP** driven by multivalent ionic pairing electrostatic attraction. Dialysis experiments using a membrane filter (molecular weight cut-off: 2.0 kDa) for the solution of **CBSP** ([**T1**] = 0.1 mM) and $Na_4[Ru(BDC)_3]$ (20 μM) showed that **CBSP** could completely suppress the diffusion of the photosensitizer,[67] which confirmed the efficient adsorption of the photosensitizer by the porous supramolecular polymer (Fig. S12†). This adsorption or inclusion would increase their efficient concentration in the interior of the polymer and thus facilitate electron transfer once the photosensitizer molecules are excited by visible light. Hydrogen evolution reaction (HER) experiments were then conducted by irradiating an aqueous solution (2 mL) that contained **PS** (20 μM), **POM** (2 μM) and **CBSP** at different concentrations. The results are presented in Table 1. In the absence of **CBSP**, the turnover number (TON) for the HER was determined to be 43 (entry 1). Adding 25, 50 and 100 μM **CBSP** could improve the TON to 208, 538 and 1683 (entries 2–4), respectively, which represents a 4.8, 12.5 and 39.1-fold increase of the TON. Further addition of **CBSP** did not cause the increase of the TON (entries 5 and 6), which may be rationalized by considering that both **PS** and **POM** had been completely included in the interior of **CBSP** and further addition of **CBSP** would rather decrease the apparent concentration of **PS** and **POM** in its interior. With the addition of **SP** at 100 μM, the TON was determined to be 78 (entry 7), which indicated that **SP** (**T1**) only slightly promoted the catalytic efficiency of the **PS-POM** system. The important confinement effect displayed by **CBSP** should reasonably reflect its increased stability and probably the pore rigidity due to the encapsulation of CB[8] for **T1**. When **M1** or its 1 : 1 mixture with CB[8] was added at an identical concentration of the donor and acceptor, the TON was found to be 36 and 61 (entries 8 and 9). Given their high concentration, these results showed that they did not impose significant influence on the catalysis of the **PS-POM** system.

Table 1 Visible light-induced proton reduction into hydrogen gas in the presence of **CBSP** or the control compound or the mixture[a]

Entry	CBSP or control	Conc.[b] (μM)	Time (h)	PS (μM)	POM (μM)	TON[c]
1	**CBSP**	0	24	20	2	43
2	**CBSP**	25	24	20	2	208
3	**CBSP**	50	24	20	2	538
4	**CBSP**	100	24	20	2	1683
5	**CBSP**	150	24	20	2	1323
6	**CBSP**	200	24	20	2	987
7	**SP**	100	24	20	2	78
8	**M1**	400	24	20	2	36
9	**M1** + CB[8]	400	24	20	2	61

[a] The hydrogen evolution reaction was conducted under irradiation of a xenon lamp (300 W, light power density: 200 mW cm^{-2}) for 24 h in the acid solution (pH = 1.8) containing methanol (20%, v/v) with a total volume of 2.0 mL. [b] For **CBSP**, referred to as [**T1**]. [c] TON determined by analysing the headspace gas with GC.

It has been reported that the bipyridinium radical cation (BIPY$^{\bullet+}$) can produce reactive oxygen species (ROS) in the presence of aerobic O_2.[71] We thus further studied the potential of **CBSP** for photocatalytic aerobic oxidation of organic sulfides to sulfoxide derivatives, for which L-methionine (**Met-S**) was used as a model substrate. The photocatalytic oxidation of **Met-S** to the sulfoxide derivative **Met-S═O** has been recently investigated by Stoddart *et al.* with BIPY-derived [2]catenane as a catalyst.[72] Under the standard reaction conditions, no oxidation of **Met-S** took place. In the presence of **CBSP** (10 mol%), the reaction proceeded smoothly (Table 2, entries 1–7). After 18 h, 90% of **Met-S** was consumed to afford **Met-S═O** in 88% yield. When the reaction time was ≤18 h, no sulfone derivative was detected from the reaction. When the reaction time was increased to 24 h, **Met-S** could be consumed completely, but the yield of **Met-S═O** was reduced to 74%, due to further oxidation of **Met-S═O** to the corresponding sulfone derivative which was confirmed by observing the formation of the sulfone derivative. In the presence of **SP** with an identical concentration (10 mol%) of **T1**, irradiating the solution for 18 h led to 68% consumption of **Met-S** and **Met-S═O** was produced in 65% yield (Table 2, entry 8). Clearly, the formation of the BIPY$^{\bullet+}$ radical cations by **CBSP** through visible light-induced electron transfer from **Met-S** was more efficient than that by **SP**. That is, **CBSP** also exhibited an important confinement effect for this organic transformation as compared with **SP**. With the decrease in the amount of both **SP** and **CBSP**, the corresponding yield of **Met-S═O** was reduced (Table 2, entries 9–12). However, **CBSP** consistently displayed higher catalytic activity. With an identical BIPY^{2+} concentration (40 mol%), **M1** or its 1 : 1 mixture with CB[8] only caused very low conversion of **Met-S** and the formation of **Met-S═O** (Table 2, entries 13 and 14). All the results are consistent with those revealed above for the photocatalytic reduction of protons to hydrogen, again supporting the important confinement effect of **CBSP**. In water, **CBSP** should not be able to adsorb hydrophilic **Met-S** in its interior. Thus, this confinement effect might be rationalized by considering that **CBSP** produces a high local concentration of BIPY^{2+} units in the supramolecular polymer, which facilitated its single electron reduction to BIPY$^{\bullet+}$ by **Met-S** molecules in the interior of the supramolecular polymer and subsequent electron transfer from BIPY$^{\bullet+}$ to O_2 to produce $O_2^{\bullet-}$. In this way, the oxidation of **Met-S** could be accelerated remarkably in the interior of **CBSP**.

Table 2 Oxidation of L-methionine in the presence of **CBSP** or different controls[a]

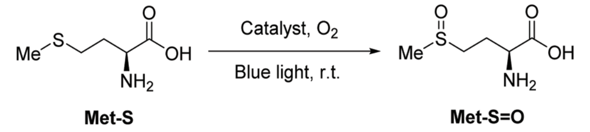

Entry	**CBSP** or control	Amount (mol%)	Time (h)	**Met-S** Conv.[b] (%)	**Met-S═O**[b] Yield (%)
1	**CBSP**	10	6	29	26
2	**CBSP**	10	9	53	46
3	**CBSP**	10	12	67	59
4	**CBSP**	10	15	75	71
5	**CBSP**	10	18	90	88
6	**CBSP**	10	21	93	79
7	**CBSP**	10	24	100	74
8	**SP (T1)**	10	18	68	65
9	**CBSP**	5	24	43	34
10	**SP (T1)**	5	24	15	12
11	**CBSP**	2.5	24	31	22
12	**SP (T1)**	2.5	24	10	8
13	**M1**	40	18	8	7
14	**M1** + CB[8]	40	18	12	9

[a] Standard reaction conditions: **Met-S** (5 mmol), **CBSP** (0.5 mmol, 10%) in H_2O (2 mL), irradiation with a blue LED strip (total 18 W, light power density: 7 mW cm^{-2}) under an aerobic oxygen atmosphere at 25 °C. [b] The conversion of **Met-S** and the yield of **Met-S═O** were determined by HPLC.

Conclusions

In summary, we have demonstrated that the cucurbit[8]uril encapsulation-based 2 + 2 donor–acceptor binding pattern can be utilized to construct a highly stable, water-soluble 3D porous supramolecular polymer from a tetrahedral building block. The new supramolecular polymer possesses a nanoscale size at micromolar scale concentrations. The new porous supramolecular polymer has been revealed to exhibit a remarkable confinement effect not only for visible light-induced proton reduction to hydrogen gas by simultaneously including a ruthenium complex photosensitizer and a polyoxometalate catalyst, but also for aerobic oxygen oxidation of methionine thioether to the corresponding sulfoxide derivative. This work opens up a new possibility for the application of the cucurbit[8] encapsulation-based 2 + 2 binding pattern to fabricate functional supramolecular architectures.

Conflicts of interest

There are no conflicts to declare.

Author contributions

ZTL and DWZ conceptualized the ideas and supervised the investigation. ZL, QL, JDS, ZKW and HW performed the experiments and collected the data. ZL and ZTL analysed the data. ZL wrote the original draft. ZTL and DWZ finished the writing. All authors read and contributed to the revisions.

Acknowledgements

We are grateful to the National Natural Science Foundation of China (Project No. 21921003, 21890730 and 21890732) for the financial support of this work.

Notes and references

1 J.-M. Lehn, Supramolecular polymer chemistry—scope and perspectives, *Polym. Int.*, 2002, **51**, 825–839.

2 L. Brunsveld, B. J. B. Folmer, E. W. Meijer and R. P. Sijbesma, Supramolecular Polymers, *Chem. Rev.*, 2001, **101**, 4071–4098.

3 S.-L. Li, T. Xiao, C. Lin and L. Wang, Advanced supramolecular polymers constructed by orthogonal self-assembly, *Chem. Soc. Rev.*, 2012, **41**, 5950–5968.

4 E. A. Appel, J. del Barrio, X. J. Loh and O. A. Scherman, Supramolecular polymeric hydrogels, *Chem. Soc. Rev.*, 2012, **41**, 6195–6214.

5 L. Yang, X. Tan, Z. Wang and X. Zhang, Supramolecular Polymers: Historical Development, Preparation, Characterization, and Functions, *Chem. Rev.*, 2015, **115**, 7196–7239.

6 G. Yu, X. Yan, C. Han and F. Huang, Characterization of supramolecular gels, *Chem. Soc. Rev.*, 2013, **42**, 6697–6722.

7 D.-W. Zhang, H. Wang and Z.-T. Li, Water-soluble Regular Three-dimensional Supramolecular and Covalent Organic Polymers, *Chem. J. Chin. Univ.*, 2020, **41**, 1139–1150.

8 T. Aida and E. W. Meijer, Supramolecular Polymers – we've Come Full Circle, *Isr. J. Chem.*, 2020, **60**, 33–47.

9 M. F. J. Mabesoone, A. R. A. Palmans and E. W. Meijer, Solute–Solvent Interactions in Modern Physical Organic Chemistry: Supramolecular Polymers as a Muse, *J. Am. Chem. Soc.*, 2020, **142**, 19781–19798.

10 R. Li, W. Chen, Y. Yang, H. Li, F. Xu, Z. Duan, T. Liang, H. Wen and W. Tian, Architecture transition of supramolecular polymers through hierarchical self-assembly: from supramolecular polymers to fluorescent materials, *Polym. Chem.*, 2020, **11**, 5642–5648.

11 T. D. Clemons and S. I. Stupp, Design of materials with supramolecular polymers, *Prog. Polym. Sci.*, 2020, **111**, 101310.

12 C. Fouquey, J.-M. Lehn and A.-M. Levelut, Molecular recognition directed self-assembly of supramolecular liquid crystalline polymers from complementary chiral components, *Adv. Mater.*, 1990, **2**, 254–257.

13 R. P. Sijbesma, F. H. Beijer, L. Brunsveld, B. J. B. Folmer, J. H. K. K. Hirschberg, R. F. M. Lange, J. K. L. Lowe and E. W. Meijer, Reversible Polymers Formed from Self-Complementary Monomers Using Quadruple Hydrogen Bonding, *Science*, 1997, **278**, 1601–1604.

14 S. Chen, Z. Geng, X. Zheng, J. Xu, W. H. Binder and J. Zhu, Engineering the morphology of hydrogen-bonded comb-shaped supramolecular polymers: from solution self-assembly to confined assembly, *Polym. Chem.*, 2020, **11**, 4022–4028.

15 L. Tao, Z.-W. Luo, K. Lan, P. Wang, Y. Guan, Z. Shen and H.-L. Xie, Stimuli-responsive luminescent supramolecular polymers based on hydrogen bonding: molecular fabrication, phase structure, and controllable-rewritable behavior, *Polym. Chem.*, 2020, **11**, 6288–6294.

16 A. Winter and U. S. Schubert, Synthesis and characterization of metallo-supramolecular polymers, *Chem. Soc. Rev.*, 2016, **45**, 5311–5357.

17 Y. Zhu, W. Zheng, W. Wang and H.-B. Yang, When polymerization meets coordination-driven self-assembly: metallo-supramolecular polymers based on supramolecular coordination complexes, *Chem. Soc. Rev.*, 2021, **50**, 7395–7417.

18 Y. Han, Y. Tian, Z. Li and F. Wang, Donor–acceptor-type supramolecular polymers on the basis of preorganized molecular tweezers/guest complexation, *Chem. Soc. Rev.*, 2018, **47**, 5165–5176.

19 T. Haino, Designer supramolecular polymers with specific molecular recognitions, *Polym. J.*, 2019, **51**, 303–318.

20 X. Ma and H. Tian, Stimuli-Responsive Supramolecular Polymers in Aqueous Solution, *Acc. Chem. Res.*, 2014, **47**, 1971–1981.

21 A. Harada, Y. Takashima and H. Yamaguchi, Cyclodextrin-based supramolecular polymers, *Chem. Soc. Rev.*, 2009, **38**, 875–882.

22 H. D. Correia, S. Chowdhury, A. P. Ramos, L. Guy, G. J.-F. Demets and C. Bucher, Dynamic supramolecular polymers built from cucurbit[n]urils and viologens, *Polym. Int.*, 2019, **68**, 572–588.

23 M. Wathier and M. W. Grinstaff, Synthesis and Properties of Supramolecular Ionic Networks, *J. Am. Chem. Soc.*, 2008, **130**, 9648–9649.

24 H. Yoon, E. J. Dell, J. L. Freyer, L. M. Campos and W.-D. Jang, Polymeric supramolecular assemblies based on multivalent ionic interactions for biomedical applications, *Polymer*, 2014, **55**, 453–464.

25 Q. Qi, B. Yang, H. Wang, D.-W. Zhang and Z.-T. Li, Supramolecular polymers from coronene multicarboxylates and multipyridiniums in water stabilized by ion-pair attraction and aromatic stacking, *Tetrahedron*, 2018, **74**, 2792–2796.

26 W. Zhao, J. Tropp, B. Qiao, M. Pink, J. D. Azoulay and A. H. Flood, Tunable Adhesion from Stoichiometry-Controlled and Sequence-Defined Supramolecular Polymers Emerges Hierarchically from Cyanostar-Stabilized Anion–Anion Linkages, *J. Am. Chem. Soc.*, 2020, **142**, 2579–2591.

27 W. Han, W. Xiang, Q. Li, H. Zhang, Y. Yang, J. Shi, Y. Ji, S. Wang, X. Ji, N. M. Khashab and J. L. Sessler, Water compatible supramolecular polymers: recent progress, *Chem. Soc. Rev.*, 2021, **50**, 10025–10043.

28 Y. Chen, S. Sun, D. Lu, Y. Shi and Y. Yao, Water-soluble supramolecular polymers constructed by macrocycle-based host-guest interactions, *Chin. Chem. Lett.*, 2019, **30**, 37–43.

29 E. Krieg, M. M. C. Bastings, P. Besenius and B. Rybtchinski, Supramolecular Polymers in Aqueous Media, *Chem. Rev.*, 2016, **116**, 2414–2477.

30 J. Tian, L. Zhang, H. Wang, D.-W. Zhang and Z.-T. Li, Supramolecular polymers and networks driven by cucurbit[8]uril-guest pair encapsulation in water, *Supramol. Chem.*, 2016, **28**, 769–783.

31 Y. Liu, H. Yang, Z. Wang and X. Zhang, Cucurbit[8]uril-Based Supramolecular Polymers, *Chem. – Asian J.*, 2013, **8**, 1626–1632.

32 H. Zou, J. Liu, Y. Li, X. Li and X. Wang, Cucurbit[8]uril-Based Polymers and Polymer Materials, *Small*, 2018, **14**, 1802234.

33 Z. Hou, W. M. Nau and R. Hoogenboom, Reversible covalent locking of a supramolecular hydrogel *via* UV-controlled anthracene dimerization, *Polym. Chem.*, 2021, **12**, 307–315.

34 S. J. Barrow, S. Kasera, M. J. Rowland, J. del Barrio and O. A. Scherman, Cucurbituril-Based Molecular Recognition, *Chem. Rev.*, 2015, **115**, 12320–12406.

35 C.-C. Zhang, X. Liu, Y.-P. Liu and Y. Liu, Two-Dimensional Supramolecular Nanoarchitectures of Polypseudorotaxanes Based on Cucurbit[8]uril for Highly Efficient Electrochemical Nitrogen Reduction, *Chem. Mater.*, 2020, **32**, 8724–8732.

36 C.-C. Zhang, Y.-M. Zhang, Z.-Y. Zhang, X. Wu, Q. Yu and Y. Liu, Photoreaction-driven two-dimensional periodic polyrotaxane-type supramolecular nanoarchitecture, *Chem. Commun.*, 2019, **55**, 8138–8141.

37 Y. Huo, Z. He, C. Wang, L. Zhang, Q. Xuan, S. Wei, Y. Wang, D. Pan, B. Dong, R. Wei, N. Naik and Z. Guo, The recent progress of synergistic supramolecular polymers: preparation, properties and applications, *Chem. Commun.*, 2021, **57**, 1413–1429.

38 W. Feng, M. Jin, K. Yang, Y. Pei and Z. Pei, Supramolecular delivery systems based on pillararenes, *Chem. Commun.*, 2018, **54**, 13626–13640.

39 R. Dong, Y. Zhou, X. Huang, X. Zhu, Y. Lu and J. Shen, Functional Supramolecular Polymers for Biomedical Applications, *Adv. Mater.*, 2015, **27**, 498–526.

40 W. Yasen, R. Dong, A. Aini and X. Zhu, Recent advances in supramolecular block copolymers for biomedical applications, *J. Mater. Chem. B*, 2020, **8**, 8219–8231.

41 L. N. Neumann, M. B. Baker, C. M. A. Leenders, I. K. Voets, R. P. M. Lafleur, A. R. A. Palmans and E. W. Meijer, Supramolecular polymers for organocatalysis in water, *Org. Biomol. Chem.*, 2015, **13**, 7711–7719.

42 E. Huerta, B. van Genabeek, B. A. G. Lamers, M. M. E. Koenigs, E. W. Meijer and A. R. A. Palmans, Triggering Activity of Catalytic Rod-Like Supramolecular Polymers, *Chem. – Eur. J.*, 2015, **21**, 3682–3690.

43 J. Tian, H. Wang, D.-W. Zhang, Y. Liu and Z.-T. Li, Supramolecular organic frameworks (SOFs): homogeneous regular 2D and 3D pores in water, *Natl. Sci. Rev.*, 2017, **4**, 426–436.

44 J. Tian, T.-Y. Zhou, S.-C. Zhang, S. Aloni, M. V. Altoe, S.-H. Xie, H. Wang, D.-W. Zhang, X. Zhao, Y. Liu and Z.-T. Li, Three-dimensional periodic supramolecular organic framework ion sponge in water and microcrystals, *Nat. Commun.*, 2014, **5**, 5574.

45 J. Tian, L. Chen, D.-W. Zhang, Y. Liu and Z.-T. Li, Supramolecular organic frameworks: engineering periodicity in water through host–guest chemistry, *Chem. Commun.*, 2016, **52**, 6351–6362.

46 Y. H. Ko, K. Kim, E. Kim and K. Kim, Exclusive Formation of 1:1 and 2:2 Complexes between Cucurbit[8]uril and Electron Donor-acceptor Molecules Induced by Host-stabilized Charge-transfer Interactions, *Supramol. Chem.*, 2007, **19**, 287–293.

47 S. Chakrabarti and L. Isaacs, Cucurbit[8]uril Controls the Folding of Cationic Diaryl Ureas in Water, *Supramol. Chem.*, 2008, **20**, 191–199.

48 G. Wu, M. Olesińska, Y. Wu, D. Matak-Vinkovic and O. A. Scherman, Mining 2:2 Complexes from 1:1 Stoichiometry: Formation of Cucurbit[8]uril–Diarylviologen Quaternary Complexes Favored by Electron-Donating Substituents, *J. Am. Chem. Soc.*, 2017, **139**, 3202–3208.

49 B. Yang, S.-B. Yu, H. Wang, D.-W. Zhang and Z.-T. Li, 2:2 Complexes from Diphenylpyridiniums and Cucurbit[8]uril: Encapsulation-Promoted Dimerization of Electrostatically Repulsing Pyridiniums, *Chem. – Asian J.*, 2018, **13**, 1312–1317.

50 G. Wu, Y. J. Bae, M. Olesińska, D. Antón-García, I. Szabó, E. Rosta, M. R. Wasielewski and O. A. Scherman, Controlling the structure and photophysics of fluorophore dimers using multiple cucurbit[8]uril clampings, *Chem. Sci.*, 2020, **11**, 812–825.

51 X. Yang, R. Wang, A. Kermagoret and D. Bardelang, Oligomeric Cucurbituril Complexes: from Peculiar Assemblies to Emerging Applications, *Angew. Chem., Int. Ed.*, 2020, **59**, 21280–21292.

52 J. D. Badjić, A. Nelson, S. J. Cantrill, W. B. Turnbull and J. F. Stoddart, Multivalency and Cooperativity in Supramolecular Chemistry, *Acc. Chem. Res.*, 2005, **38**, 723–732.

53 C. F. V. Sousa, E. Fernandez-Megia, J. Borges and J. F. Mano, Supramolecular dendrimer-containing layer-by-layer nanoassemblies for bioapplications: current status and future prospects, *Polym. Chem.*, 2021, **12**, 5902–5930.

54 Y. Liu, Y. Yu, J. Gao, Z. Wang and X. Zhang, Water-Soluble Supramolecular Polymerization Driven by Multiple Host-Stabilized Charge-Transfer Interactions, *Angew. Chem., Int. Ed.*, 2010, **49**, 6576–6579.

55 J. Sun, G. M. Stone, N. P. Balsara and R. N. Zuckermann, Structure–Conductivity Relationship for Peptoid-Based PEO–Mimetic Polymer Electrolytes, *Macromolecules*, 2012, **45**, 5151–5156.

56 C. Zhou, J. Tian, J.-L. Wang, D.-W. Zhang, X. Zhao, Y. Liu and Z.-T. Li, A three-dimensional cross-linking supramolecular polymer stabilized by the cooperative dimerization of the viologen radical cation, *Polym. Chem.*, 2014, **5**, 341–345.

57 F. B. L. Cougnon, N. Ponnuswamy, N. A. Jenkins, G. D. Pantoș and J. K. M. Sanders, Structural Parameters Governing the Dynamic Combinatorial Synthesis of Catenanes in Water, *J. Am. Chem. Soc.*, 2012, **134**, 19129–19135.

58 S. Hagihara, L. Gremaud, G. Bollot, J. Mareda and S. Matile, Screening of π-Basic Naphthalene and Anthracene Amplifiers for π-Acidic Synthetic Pore Sensors, *J. Am. Chem. Soc.*, 2008, **130**, 4347–4351.

59 Z.-J. Zhang, H.-Y. Zhang, L. Chen and Y. Liu, Interconversion between [5]Pseudorotaxane and [3]

Pseudorotaxane by Pasting/Detaching Two Axle Molecules, *J. Org. Chem.*, 2011, **76**, 8270–8276.

60 B. Zhang, Y. Zhang, M. Hou, W. Wang, S. Hu, W. Cen, X. Cao, S. Qiao and B.-H. Han, Pristine, metal ion and metal cluster modified conjugated triazine frameworks as electrocatalysts for hydrogen evolution reaction, *J. Mater. Chem. A*, 2021, **9**, 10146–10159.

61 Y. Yang, Y.-N. Jiang, Z.-Y. Lin, J.-H. Zeng, Z.-K. Liu and Z.-P. Zhan, Highly regio- and stereo-selective heterogeneous 1,3-diyne hydrosilylation controlled by a nickel-metalated porous organic polymer, *Org. Chem. Front.*, 2021, **8**, 4826–4832.

62 M. Xu, C. Lai, X. Liu, B. Li, M. Zhang, F. Xu, S. Liu, L. Li, L. Qin, H. Yi and Y. Fu, COF-confined catalysts: from nanoparticles and nanoclusters to single atoms, *J. Mater. Chem. A*, 2021, **9**, 24148–24174.

63 H. Zhang, L.-L. Lou, K. Yu and S. Liu, Advances in Chiral Metal Organic and Covalent Organic Frameworks for Asymmetric Catalysis, *Small*, 2021, **17**, 2005686.

64 L. Zhang, Q. Cao, F. Gao, Y. Dong and X. Li, Self-supported rhodium catalysts based on a microporous metal–organic framework for polymerization of phenylacetylene and its derivatives, *Polym. Chem.*, 2020, **11**, 2904–2913.

65 H.-K. Liu, Y.-F. Lei, P.-J. Tian, H. Wang, X. Zhao, Z.-T. Li and D.-W. Zhang, $[Fe(bpy)_3]^{2+}$-based porous organic polymers with boosted photocatalytic activity for recyclable organic transformations, *J. Mater. Chem. A*, 2021, **9**, 6361–6367.

66 J. Tian, Z.-Y. Xu, D.-W. Zhang, H. Wang, S.-H. Xie, D.-W. Xu, Y.-H. Ren, H. Wang, Y. Liu and Z.-T. Li, Supramolecular metal-organic frameworks that display high homogeneous and heterogeneous photocatalytic activity for H2 production, *Nat. Commun.*, 2016, **7**, 11580.

67 S.-B. Yu, Q. Qi, B. Yang, H. Wang, D.-W. Zhang, Y. Liu and Z.-T. Li, Enhancing Hydrogen Generation Through Nanoconfinement of Sensitizers and Catalysts in a Homogeneous Supramolecular Organic Framework, *Small*, 2018, **14**, 1801037.

68 Y.-C. Zhang, Z.-Y. Xu, Z.-K. Wang, H. Wang, D.-W. Zhang, Y. Liu and Z.-T. Li, A Woven Supramolecular Metal-Organic Framework Comprising a Ruthenium Bis(terpyridine) Complex and Cucurbit[8]uril: Enhanced Catalytic Activity toward Alcohol Oxidation, *ChemPlusChem*, 2020, **85**, 1498–1503.

69 Z.-Z. Gao, Z.-K. Wang, L. Wei, G. Yin, J. Tian, C.-Z. Liu, H. Wang, D.-W. Zhang, Y.-B. Zhang, X. Li, Y. Liu and Z.-T. Li, Water-Soluble 3D Covalent Organic Framework that Displays an Enhanced Enrichment Effect of Photosensitizers and Catalysts for the Reduction of Protons to H_2, *ACS Appl. Mater. Interfaces*, 2020, **12**, 1404–1411.

70 H. Lv, J. Song, H. Zhu, Y. V. Geletii, J. Bacsa, C. Zhao, T. Lian, D. G. Musaev and C. L. Hill, Visible-light-driven hydrogen evolution from water using a noble-metal-free polyoxometalate catalyst, *J. Catal.*, 2013, **307**, 48–54.

71 E. J. Nanni, C. T. Angelis, J. Dickson and D. T. Sawyer, Oxygen activation by radical coupling between superoxide ion and reduced methyl viologen, *J. Am. Chem. Soc.*, 1981, **103**, 4268–4270.

72 Y. Jiao, L. Đorđević, H. Mao, R. M. Young, T. Jaynes, H. Chen, Y. Qiu, K. Cai, L. Zhang, X.-Y. Chen, Y. Feng, M. R. Wasielewski, S. I. Stupp and J. F. Stoddart, A Donor–Acceptor [2]Catenane for Visible Light Photocatalysis, *J. Am. Chem. Soc.*, 2021, **143**, 8000–8010.